Am J Physiol Heart Circ Physiol 294: H613–H621, 2008.
First published December 7, 2007; doi:10.1152/ajpheart.01332.2007.

Characterization of the phospholemman knockout mouse heart: depressed left ventricular function with increased Na-K-ATPase activity

James R. Bell,[1]* Erika Kennington,[1]* William Fuller,[1] Kushal Dighe,[1] Pamela Donoghue,[2] James E. Clark,[1] Li-Guo Jia,[3] Amy L. Tucker,[3] J. Randall Moorman,[3] Michael S. Marber,[1] Philip Eaton,[1] Michael J. Dunn,[2] and Michael J. Shattock[1]

[1]*Cardiovascular Division, King's College London, Rayne Institute, St Thomas' Hospital, London, United Kingdom;* [2]*Proteome Research Centre, Conway Institute of Biomolecular and Biomedical Research, University College Dublin, Belfield, Dublin, Ireland; and* [3]*Cardiovascular Division, Department of Internal Medicine, University of Virginia Health Sciences Center, Charlottesville, Virginia*

Submitted 13 November 2007; accepted in final form 3 December 2007

Bell JR, Kennington E, Fuller W, Dighe K, Donoghue P, Clark JE, Jia LG, Tucker AL, Moorman JR, Marber MS, Eaton P, Dunn MJ, Shattock MJ. Characterization of the phospholemman knockout mouse heart: depressed left ventricular function with increased Na-K-ATPase activity. *Am J Physiol Heart Circ Physiol* 294: H613–H621, 2008. First published December 7, 2007; doi:10.1152/ajpheart.01332.2007.—Phospholemman (PLM, FXYD1), abundantly expressed in the heart, is the primary cardiac sarcolemmal substrate for PKA and PKC. Evidence supports the hypothesis that PLM is part of the cardiac Na-K pump complex and provides the link between kinase activity and pump modulation. PLM has also been proposed to modulate Na/Ca exchanger activity and may be involved in cell volume regulation. This study characterized the phenotype of the PLM knockout (KO) mouse heart to further our understanding of PLM function in the heart. PLM KO mice were bred on a congenic C57/BL6 background. In vivo conductance catheter measurements exhibited a mildly depressed cardiac contractile function in PLM KO mice, which was exacerbated when hearts were isolated and Langendorff perfused. There were no significant differences in action potential morphology in paced Langendorff-perfused hearts. Depressed contractile function was associated with a mild cardiac hypertrophy in PLM KO mice. Biochemical analysis of crude ventricular homogenates showed a significant increase in Na-K-ATPase activity in PLM KO hearts compared with wild-type controls. SDS-PAGE and Western blot analysis of ventricular homogenates revealed small, nonsignificant changes in Na-K-ATPase subunit expression, with two-dimensional gel (isoelectric focusing, SDS-PAGE) analysis revealing minimal changes in ventricular protein expression, indicating that deletion of PLM was the primary reason for the observed PLM KO phenotype. These studies demonstrate that PLM plays an important role in the contractile function of the normoxic mouse heart. Data are consistent with the hypothesis that PLM modulates Na-K-ATPase activity, indirectly affecting intracellular Ca and hence contractile function.

FXYD1; contractile function; intracellular sodium regulation

IN EXCITABLE TISSUES, the activity of the plasma membrane Na-K-ATPase is vital for the maintenance of normal electrical activity, ionic homeostasis, cell volume control, and substrate and amino acid transport and for setting cellular Ca load and hence contractility. Interventions that influence Na-K-ATPase activity and/or the transmembrane Na gradient can therefore profoundly affect myocardial function. In essence, the Na-K-ATPase not only influences a wide range of transmembrane transport processes but also indirectly controls myocardial contractility.

It has recently been recognized that the FXYD family of small single transmembrane-spanning proteins are tissue-specific regulators of the Na-K-ATPase (3–5, 28). Phospholemman (PLM, FXYD1) is expressed in excitable tissues and is unique among the FXYD proteins in that it contains a cytoplasmic region with consensus phosphorylation sites for kinases that include PKC and PKA (21, 30). In fact, PLM was originally identified as the primary sarcolemmal substrate for PKA and PKC phosphorylation in the heart (10, 23, 24). We have shown (6, 15, 17, 26) that PLM forms an integral part of the cardiac Na-K pump complex and provides the link between kinase activation and pump modulation. Elevation of cAMP [as occurs in isoprenaline (Iso)-induced β-receptor stimulation] activates cAMP-dependent kinase (PKA), which in turn phosphorylates Ser68 on PLM (26). This not only disinhibits the Na-K pump but actually stimulates activity, raising V_{max} by ~35% and increasing the sensitivity of the pump to intracellular Na (6). This stimulatory effect of Iso on the pump is absent in PLM knockout (KO) mice (6). A recent paper from Han et al. (19) also reports a PKC-mediated increase in V_{max}, via PLM phosphorylation, independent of a change in Na affinity.

In 2005 Tucker and colleagues (20) generated and described a mouse in which the gene encoding PLM was selectively deleted. This mouse, generated on a noncongenic background (mixed C57/BL6 and S129J), showed evidence of mild cardiac hypertrophy, increased ejection fraction, a decrease in Na-K-ATPase activity (measured as enzymatic ATP hydrolysis), and decreased Na-K-ATPase protein expression. However, electrophysiological studies of myocytes isolated from PLM KO mice that had been rederived on a congenic C57/BL6 background conversely showed increased Na-K pump current in KO myocytes (13). This suggests that at least some of the initial phenotypic observations in the original PLM mouse line may have been related to the noncongenic background rather than the specific gene deletion. To address this issue, we have undertaken an extensive characterization of the rederived PLM KO mouse cardiac phenotype. These studies provide insight into the role of PLM in cardiac physiology and lay the

* J. R. Bell and E. Kennington contributed equally to these studies.

Address for reprint requests and other correspondence: M. J. Shattock, Cardiac Physiology, King's College London, Cardiovascular Division, Rayne Institute, St Thomas' Hospital, London SE1 7EH (e-mail: michael.shattock@kcl.ac.uk).

The costs of publication of this article were defrayed in part by the payment of page charges. The article must therefore be hereby marked "*advertisement*" in accordance with 18 U.S.C. Section 1734 solely to indicate this fact.

foundation for future studies of the role of PLM in kinase-mediated regulation of Na-K-ATPase.

MATERIALS AND METHODS

Animals. PLM KO mice were generated as previously described (20) except that they are now congenic on a pure C57BL/6 background. Briefly, a PLM KO mouse cell line was created by replacing the PLM gene (exons 3–5) with an insert containing lacZ in the AB2.2 stem cell line. Blastocyst injection and generation of germlike chimeric mice were performed in the University of Virginia Transgenic Facility. Two breeding strategies were used. In most studies, heterozygous breeding pairs were used to generate PLM KO and wild-type (WT) littermates (*strategy A*). However, to maximize efficiency, a number of homozygote (−/−) breeding pairs were established (*strategy B*). Only first-generation offspring of this breeding strategy were used, and they were compared with their WT cousins.

Animals were maintained humanely in compliance with the "Principles of Laboratory Animal Care" formulated by the National Society for Medical Research and the *Guide for Care and Use of Laboratory Animals* prepared by the National Academy of Sciences and published by the National Institutes of Health (NIH Pub. No. 85-23, revised 1985). All animal protocols were approved both by the local King's College Ethical Review Process Committee and by the UK Government Home Office (Animals Scientific Procedures Group).

In vivo conductance catheter measurements. Age-matched young adult male PLM KO and WT mice (15.3 ± 0.9 and 15.0 ± 0.6 wk, respectively; $n = 8$) were anesthetized with ketamine, medetomidine, and atropine (100, 0.2, and 0.4 mg/kg, respectively) and placed on a heated pad. A rectal probe was inserted, and mouse core temperature was maintained at 37°C. Mice were ventilated through a tracheostomy with a MiniVent ventilator (Harvard Apparatus) set to a tidal volume of 235 μl at a rate of 105 breaths/min. A transverse substernal incision was performed, and the muscle was cauterized to prevent blood loss. After cauterization of the diaphragm, the left ventricular apex was exposed and punctured with a 26-gauge needle, creating a hole for the pressure-volume probe to be inserted. An SPR-839 Millar 1.4-F catheter, connected to MPCU-200 P-V signal conditioning hardware (Millar Instruments, Houston, TX), was inserted into the left ventricle, with combined pressure and volume signals used to generate pressure-volume loops for determination of cardiac function and hemodynamic analysis. The heart was allowed to stabilize for 5 min after insertion of the probe, to allow the pressure trace to settle to a steady state. At the end of the experiment, 10 μl of 15% hypertonic saline solution was injected into the external jugular vein and the parallel conductance of the myocardial tissue was determined to reveal the intraventricular blood volumes.

Isolated heart preparation. Age-matched young adult mice [11.0 ± 0.9 wk ($n = 6$) vs. 11.6 ± 0.7 wk ($n = 7$); P = not significant (ns)] were anesthetized with pentobarbital sodium in combination with heparin sodium (200 mg/kg and 200 IU/kg, respectively, ip). Hearts were rapidly excised and placed in cold (4°C) bicarbonate buffer, and the aorta was cannulated with a "blunted" 21-gauge needle. Hearts were then perfused with oxygenated (95% O_2-5% CO_2) bicarbonate buffer at 37.0°C (pH 7.4). Perfusion was in the nonrecirculating Langendorff mode at a constant pressure equivalent to 80 mmHg, and, unless stated otherwise, hearts were paced at 540 beats per minute (bpm). The bicarbonate buffer contained (in mM) 118.5 NaCl, 4.7 KCl, 1.18 KH_2PO_4, 25.0 $NaHCO_3$, 1.2 $MgCl_2$, 1.4 $CaCl_2$, 11.1 glucose, and 2.0 sodium pyruvate. Left ventricular developed pressure (LVDP) measurements were performed with a fluid-filled balloon inflated to give an end-diastolic pressure of ~5–9 mmHg.

Effect of Ca concentration on LVDP in Langendorff-perfused PLM knockout hearts. PLM WT and KO hearts ($n = 6$) were perfused for 20 min in Krebs-Henseleit bicarbonate buffer (KHB) containing 1.4 mM Ca and paced at 540 bpm, and LVDP was recorded with an intraventricular balloon. The perfusate was subsequently switched to KHB containing either 0.55 mM Ca or 3.5 mM Ca, and contractile function was recorded after 3 min. Data are expressed as means ± SE for each genotype.

Monophasic action potential recording. Isolated mouse hearts were paced via bipolar silver/silver chloride electrodes placed on the apex of the left ventricle at 540 bpm, and the noise and stimulus artifact on the monophasic action potential electrode was minimized by using an optically isolated stimulator, a pulse width of 0.1 ms, and voltage just greater than threshold. Monophasic action potentials were recorded from the epicardial left ventricular free wall with a miniaturized suction electrode (12).

Na-K-ATPase activity studies. Na-K-ATPase activity measurements, based on the method of Baginski et al. (2), were performed on PLM WT and KO ventricular homogenates. Hearts from PLM WT and KO mice (WT $n = 7$ and KO $n = 5$) were aerobically perfused for 30 min to wash the blood out of the coronary vasculature. Ventricles were removed, weighed, and stored in liquid nitrogen. Homogenates (0.5% wt/vol) were prepared in SET buffer (mM: 0.315 sucrose, 1 EDTA, 20 Tris pH 7.5) containing protease inhibitors (Complete EDTA-Free Protease Inhibitor Cocktail Tablets, Roche) with a ground glass tissue grinder at 4°C. Equal volumes of homogenate and 2× SDS sample buffer were combined for subsequent analysis by SDS-PAGE and Western blotting. Ten microliters of cardiac sample was added to 0.5 ml of reaction buffer (mM: 25 histidine pH 7.5, 130 NaCl, 20 KCl, 3 $MgCl_2$ ± 10 ouabain) and prewarmed to 37°C. The reaction was initiated with 3 mM ATP, incubated for 5 min at 37°C, and terminated with the addition of 0.5 ml of 4°C stop buffer (0.5 M HCl, 30 mg/ml ascorbic acid, 5 mg/ml ammonium heptamolybdate, 10 mg/ml SDS). Color was developed with the addition of 0.75 ml of development solution [20 mg/ml sodium (meta)arsenite, 20 mg/ml sodium citrate, 20 μl/ml acetic acid] at 37°C and incubated for 10 min at 37°C. All reactions were performed in duplicate. The absorbance at 850 nm (A_{850}) of the phosphomolybdate complex of each sample was subsequently measured with a spectrophotometer (CamSpec M330 Spectrophotometer, Cambridge, UK; $\lambda = 850$ nm). The amount of phosphate produced (nmol) was determined with a calibration curve performed with increasing amounts of Na_3PO_4 added to the reaction buffer.

Protein analysis and Western blotting. Hearts from PLM WT and KO mice were aerobically perfused for 30 min ($n = 8$) to wash the blood out of the coronary vasculature. Ventricles were removed, weighed, and stored in liquid nitrogen. Ventricles were subsequently thawed, homogenized with a motor-driven blade (Ystral Drive X10/25, Ballrechten-Dottingen) in a HEPES-sucrose buffer (10% wt/vol; mM: 20 HEPES pH 7.4, 250 sucrose, 2 EDTA, 1 $MgCl_2$) at 4°C and added to an equal volume of 2× SDS sample buffer for analysis by SDS-PAGE and Western blotting, as described previously (16).

Antibodies. Primary antibodies used in these studies included Na-K-ATPase α_1-subunit (α6F, Univ. of Iowa Hybridoma Bank), α2-subunit (06-168, Upstate), α_3-subunit (SA247, Affiniti Research Products), total α-subunit (α5, Univ. of Iowa Hybridoma Bank), β_1-subunit (06-170, Upstate), β_2-subunit (06-1171, Upstate), phospholemman (C2 antibody) (25), Na/Ca exchanger (MA3-926, Affinity Bioreagents), sarco(endo)plasmic reticulum Ca-ATPase (SERCA)2a (MA3-919, Affinity Bioreagents), phospholamban (05-205, Upstate), α_{1c} dihydropyridine receptor (ACC-003, Alomone Labs) and α-myosin heavy chain (HV11, Univ. of Iowa Hybridoma Bank).

Two-dimensional electrophoresis. PLM WT and KO hearts ($n = 5$) were aerobically perfused in the Langendorff mode for 30 min and frozen in liquid nitrogen. Hearts were homogenized and subjected to a standard two-dimensional electrophoresis protocol [isoelectric focusing (IEF) and SDS-PAGE] as described previously (14, 32). Briefly, ventricular samples were ground under liquid nitrogen, incubated in 1 ml of differential gel electrophoresis (DIGE)-compatible lysis buffer [9.5 M urea, 2% 3-[(3-cholamidopropyl)dimethylammonio]-1-propanesulfonate (CHAPS) (wt/vol), and 20 mM Tris pH 8.0–8.5] at room temperature for 1 h, and then sonicated on ice and

centrifuged for 30 min at 14,000 g_{av} to produce protein fractions. All preparative steps were performed at 0–4°C in the presence of a protease inhibitor (Roche complete protease inhibitor cocktail tablets) to prevent proteolytic degradation. Protein concentration was determined with the Bradford dye binding assay (11). Minimal CyDye labeling (GE Healthcare) was performed at a concentration of 25 μg of protein/200 pmol of CyDye for two-dimensional electrophoresis. Labeled samples were incubated on ice for 30 min in the dark, and the labeling reaction was terminated by the addition of 10 mM lysine. Samples were then centrifuged briefly and incubated on ice in the dark for a further 10 min. Protein samples were combined with an equal volume of 2× lysis buffer (9.5 M urea, 2% CHAPS, 2% DTT, and 1.6% Pharmalyte pH 3–10) followed by in-gel rehydration overnight before IEF.

Samples were subjected to IEF at 0.05 mA/IPG strip for 72,000 Vh at 20°C. The strips were equilibrated in 6 M urea containing 30% (vol/vol) glycerol, 2% (wt/vol) SDS, 0.05 M Tris·HCl pH 8.8, and 0.01% (wt/vol) bromophenol blue with the addition of 1% (wt/vol) DTT for 15 min. Subsequently, the strips were equilibrated in the same buffer without DTT but with the addition of 4.8% (wt/vol) iodoacetamide for 15 min (18). The second dimension was carried out overnight with a Bio-Rad Protean Plus Dodeca Cell system at 1 W/gel at 15°C and was terminated when the dye front had just migrated off the lower end of the gels. Gels were subsequently scanned with a Typhoon variable-mode imager 9400 (GE Healthcare), with a standard pixel volume of 40,000–60,000 for all scans.

Protein expression changes were determined with the protein expression analysis software DeCyder (GE Healthcare). All gels were matched, and spot artifacts were filtered out on the basis of volume, area, and slope. Proteins found to be significant ($P < 0.05$, ANOVA) were picked for tryptic digestion from Plus-One silver-stained micropreparative gels. Tryptic peptides were analyzed with an Applied Biosystems 4700 Proteomics Analyzer matrix-assisted laser desorption/ionization (MALDI)-time of flight (TOF)-TOF mass spectrometer using 10 mg/ml α-cyano-4-hydroxycinnamic acid as the matrix. Mass spectra were acquired in the reflector mode, and the peptide sequences were confirmed by tandem mass spectroscopy (MS)/MS of selected precursors. The precursor ion masses and the masses of the daughter ions from MS/MS experiments were scanned against the SwissProt database with Mascot Search Software incorporated in GPS Explorer version 3.5 software, with precursor tolerance set at 150 ppm and MS/MS fragment tolerance set at 0.25 Da.

Statistics. Results are presented as means ± SE. Differences between groups were assessed with two-way ANOVA followed by Student-Newman-Keuls test. Differences were considered significant at the 95% confidence level. In the studies of changes in contractility in response to changes in perfusate Ca, the mouse × extracellular Ca concentration ($[Ca]_o$) interaction was assessed with regression analysis and the statistical package STATA8 (which allows the power of the paired experimental design to be analyzed).

RESULTS

Left ventricular function in vivo. Table 1 shows the age, body weight, and ventricular weights measured in the two cohorts of mice in this in vivo study. Body weight was similar in PLM WT and KO mice. However, wet ventricular weight was significantly increased in PLM KO hearts, because of an increased left ventricular weight, and hence the total and left ventricular-to-body weight ratios were also significantly increased.

Figure 1*A* shows a series of pressure-volume loops generated in a WT mouse at a constant end-diastolic volume, and Fig. 1*B* shows a family of loops generated after inferior vena cava occlusion. Measured and calculated indexes of cardiac function derived from such measurements in WT and PLM KO mice are shown in Table 2.

Table 1. *Age and body and heart weights of PLM WT and KO mice used for in vivo conductance catheter measurements*

	WT	KO	*P* Value
Age, wk	15.3±0.9	15.0±0.6	ns
Body weight, g	30.5±1.5	29.9±0.4	ns
Total ventricular weight, mg	107±3	118±3	<0.05
Left ventricular weight, mg	83±3	93±3	<0.05
Right ventricular weight, mg	24±1	25±1	ns
Total ventricular-to-body weight ratio (×10²)	3.54±0.08	3.97±0.10	<0.005
Left ventricular-to-body weight ratio (×10²)	2.73±0.06	3.12±0.10	<0.01

Data are means ± SE (n = 8/group). Ventricular weights are wet weights. PLM, phospholemman; WT, wild type; KO, knockout; ns, not significant.

Despite no significant differences in the basic volume and pressure readings of PLM WT and KO hearts (Table 2), various derived indexes of contractile function reveal a depressed systolic and diastolic function in the PLM KO hearts. The most striking differences between the genotypes were the decreased maximum and minimum rate of change of pressure with respect to time (dP/dt_{max} and dP/dt_{min}) during the cardiac cycle in the PLM KO hearts. This was accompanied by a significantly decreased stroke work and maximum power in the PLM KO hearts. Additionally, the relaxation time constant [τ(Weiss)], a marker of diastolic relaxation, was significantly greater in the PLM KO mouse, indicating a compromised diastolic function. These parameters indicate that there is a significant depression of both systolic and diastolic function in PLM KO mice.

Left ventricular function in Langendorff-perfused hearts. Figure 2*A* shows LVDP measured in PLM KO and WT hearts over 20 min of aerobic perfusion. Hearts were paced at 540 bpm throughout the protocol. In a separate study, no effect of PLM knockout was seen on unstimulated heart rate [472 ± 14 bpm in PLM KO vs. 451 ± 17 bpm in WT (n = 6/group; P = ns)]. In the paced hearts (Fig. 2*A*), LVDP was significantly depressed throughout the aerobic perfusion in PLM KO hearts compared with WT controls. After 20-min aerobic perfusion, LVDP in PLM KO hearts (76.6 ± 4.1 mmHg) was 80% of that in WT hearts (94.8 ± 4.3 mmHg). There were no differences between genotypes in left ventricular end-diastolic pressure (LVEDP; range 6.5–8 mmHg) or coronary flow (CF; 2–3 ml/min) (data not shown).

Ca sensitivity of Langendorff-perfused PLM knockout hearts. Tucker et al. (29) reported that contractility in cardiac myocytes isolated from PLM KO mice is similar to that in WT myocytes when measured in 1.8 mM extracellular Ca. However, contractility is reduced in PLM KO myocytes at low extracellular Ca and is increased at high Ca. In this study, action potential duration was profoundly increased in KO myocytes at both 50% repolarization (prolonged by 50%) and 90% repolarization (prolonged by 250%). These studies were, however, conducted at nonphysiological pacing rates of 1 Hz and in current-clamped dialyzed myocytes. We therefore investigated the Ca dependence of contraction and action potential duration in our Langendorff-perfused hearts paced at 540 bpm and 37°C.

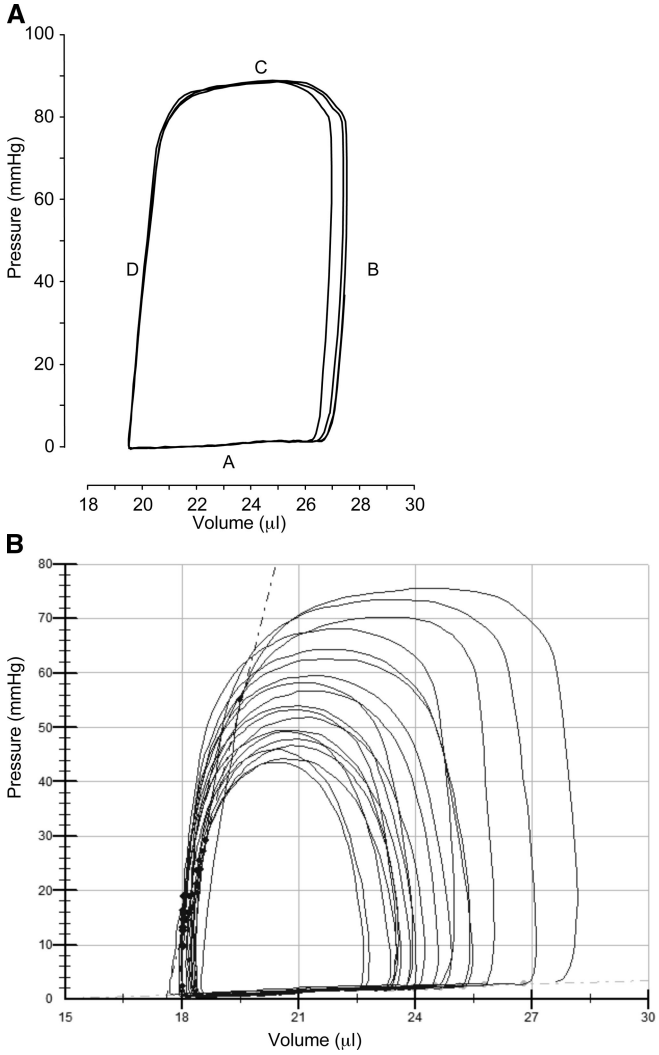

Fig. 1. Examples of pressure-volume loops produced from in vivo conductance catheters. *A*: example of a pressure-volume loop in wild-type (WT) mice. The loop is split up into 4 stages, ventricular filling (A), isovolumic contraction (B), ventricular ejection (C), and isovolumic relaxation (D), and is independent of time. *B*: series of loops after IVC occlusion. The gradients of the end-systolic and end-diastolic points in the presence of a decreasing preload, represented by the dotted vertical and horizontal lines, are used by the PV Analysis Software to calculate the end-systolic and end-diastolic pressure-volume relationships, respectively. Note that the values for the volumes include the parallel conductance, which is calculated at the end of the experiment.

Figure 2*B* shows the relationship between perfusate Ca concentration and LVDP. As described previously, Langendorff-perfused PLM KO hearts were functionally depressed compared with WT controls when perfused with physiological concentrations of Ca (1.4 mM). However, at both low and high concentrations of perfusate Ca, no significance difference in LVDP was measured between PLM WT and KO hearts.

Figure 3*A* shows representative monophasic action potentials from PLM KO and WT hearts at two Ca concentrations (1.4 and 3.5 mM). No differences in action potential morphology were detected at 1.4 or 3.5 mM Ca (for quantitative detail see Fig. 3*C*). Figure 3*B* shows the same examples as in Fig. 3*A* replotted to allow comparison of the effects of Ca within a genotype. Raising extracellular Ca is known to inhibit the inward current generated by forward mode Na/Ca exchange (the current that is largely responsible for the "foot" of the mouse action potential) (8). Consistent with this, Fig. 3, *B* and *C*, show that raising Ca to 3.5 mM shortens the action potential equally in both PLM KO and WT hearts.

Na-K-ATPase activity in ventricular homogenates. Na-K-ATPase activity was determined by normalizing ouabain-sensitive phosphate production from ATP to wet ventricular weight over the duration of a 5-min reaction. Figure 4*A* shows that Na-K-ATPase activity was significantly greater in PLM KO ventricular homogenates compared with WT controls. The Na-K-ATPase activity of the crude homogenates from PLM WT and KO hearts was subsequently normalized to total α-subunit expression in each sample to compensate for previously reported changes in α_1-subunit expression in the PLM KO cardiomyocyte (29). Figure 4*B* shows that Na-K-ATPase activity normalized to pump protein expression was more than doubled in PLM KO hearts compared with WT controls. This is consistent with observations made in voltage-clamped myocytes isolated from PLM KO hearts, where K-sensitive unitary Na-K pump current has been reported to be approximately double that measured in WT myocytes (7).

SDS-PAGE and Western blotting protein analysis. Table 3 shows that PLM was absent from the crude ventricular homogenate of PLM KO mouse hearts. Small, nonsignificant decreases in the expression of selected Na-K-ATPase subunits were observed in PLM KO ventricular homogenates compared with WT. Most notably, there was an ~25% decrease (not significant) in α_1-subunit expression in PLM KO hearts compared with WT. There were also small, nonsignificant changes in the expression of the sarcoplasmic reticulum proteins SERCA2a and phospholamban, as well as Na/Ca exchanger (NCX), in PLM KO hearts compared with WT controls.

Two-dimensional gel protein analysis. DIGE-labeled proteins from PLM WT and KO heart homogenates were focused according to isoelectric point in first-dimension IEF and subsequently by molecular weight in second-dimension SDS-PAGE to produce a proteomic profile of the PLM KO heart.

Table 2. *Functional and derived variables measured with an in vivo conductance catheter in PLM WT and KO mice*

	WT	KO	*P* Value
Heart rate, bpm	383±11	377±7	ns
P_{es}, mmHg	90±2	85±2	ns
P_{ed}, mmHg	2.3±0.2	2.4±0.2	ns
V_{ed}, μl	10.2±0.7	10.1±2.0	ns
V_{es}, μl	3.1±0.6	5.2±1.5	ns
Stroke volume, μl	7.7±0.6	6.1±1.0	ns
Ejection fraction, %	73±5	60±6	ns
Cardiac output, μl/min	2,976±250	2,281±358	ns
Stroke work, mmHg·μl	597±55	396±70	<0.05
Maximum power, mW	2.94±0.44	1.80±0.27	<0.05
dP/dt_{max}, mmHg/s	7,765±294	4,651±173	<0.001
dP/dt_{min}, mmHg/s	−7,443±256	−5,079±190	<0.001
dV/dt_{max}, μl/s	293±28	220±43	ns
dV/dt_{min}, μl/s	−267±36	−167±24	<0.05
τ(Weiss), ms	7.64±0.13	9.67±0.25	<0.001

Data are means ± SE (n = 8). P_{es}, end-systolic pressure; P_{ed}, end-diastolic pressure; V_{ed}, end-diastolic volume; V_{es}, end-systolic volume; dP/dt_{max} and dP/dt_{min}, maximum and minimum rate of change of pressure with respect to time; dV/dt_{max} and dV/dt_{min}, maximum and minimum rate of change of volume with respect to time; τ, relaxation time constant.

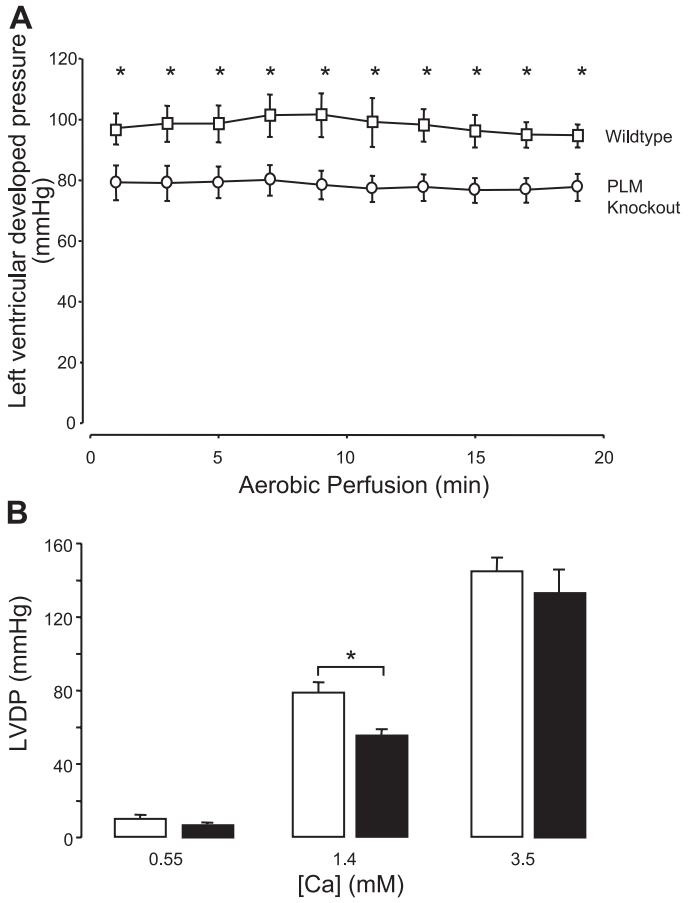

Fig. 2. Left ventricular developed pressure (LVDP) measured in Langendorff-perfused hearts isolated from phospholemman (PLM) WT and knockout (KO) mice during 20-min aerobic perfusion (*A*) and at different extracellular Ca concentrations ([Ca]) (*B*). *A*: PLM KO hearts ($n = 6$) had a significantly depressed LVDP compared with WT controls ($n = 6$) after 30 min of aerobic perfusion (*$P < 0.05$ compared with WT). Data are means ± SE. *B*: data for 1.4 mM Ca were taken after 20-min stabilization ($n = 12$), and data for both 0.55 mM and 3.5 mM Ca were taken 3 min after switching to the relevant concentration ($n = 6$). PLM KO hearts (filled bars) exhibited depressed function at physiological [Ca] (1.4 mM) compared with WT hearts (open bars) (*$P < 0.05$); however, this was not seen at either low or high [Ca]. Regression analysis of these data indicates that while Ca significantly increased LVDP in both genotypes, the rise in LVDP at 1.4 mM Ca was significantly less in the KO group compared with WT mice [PLM KO*Ca (1.4 mM); $P = 0.016$]. However, this relative difference in the increase in LVDP between WT and PLM KO mice was not seen at supraphysiological levels of Ca (3.5 mM; $P = 0.606$).

Figure 5 depicts differentially labeled PLM WT and KO homogenates with proteins of interest, as determined with DeCyder software analysis, circled and numbered 1–12 ($P < 0.05$, $n = 5$). These proteins were tryptically digested and identified by MS/MS, as described in Table 4. The majority of these were abundant proteins involved in cellular metabolism.

DISCUSSION

This study has characterized cardiac contractile function and protein expression in hearts isolated from PLM KO mice bred on a congenic C57BL/6 background. The principal findings are that PLM ablation results in a mild depression of contractility in vivo, which is more significant when hearts are isolated and Langendorff perfused. In Langendorff-perfused hearts paced at 540 bpm, there were no significant differences in action potential morphology. The depressed contractility was associated with a mild cardiac hypertrophy, an approximate doubling of normalized Na-K-ATPase activity, but no significant change in the expression of major proteins involved in excitation-contraction coupling. Two-dimensional electrophoresis provided the first proteomic screen of the PLM KO heart and revealed minimal changes in protein expression, principally in mitochondrial enzymes.

The decline in left ventricular function, measured both in vivo and in vitro, suggests that deletion of PLM affects cardiac contractility. Since PLM deletion was also shown in this study, and in others (7, 13), to increase unitary Na-K-ATPase activity, a simple explanation for the decline in contractility could be that this is secondary to a decreased intracellular Na concentration in PLM KO hearts. This would be consistent with our observation that this depression in contractility could be rescued at high $[Ca]_o$ with near maximally activated LVDP similar in WT and PLM KO hearts. Despa et al. (13) directly measured intracellular Na with the Na-sensitive fluorescent probe Na-binding benzofuran isophthalate (SBFI) in quiescent mouse myocytes at room temperature and found no differences between PLM KO and WT cells. However, since Na influx is likely to be low in a quiescent myocyte at room temperature the important question is, what is the effect of PLM deletion on intracellular Na in a rapidly beating heart at 37°C? Unfortunately, at present the use of Na-sensitive fluorescent probes is largely limited to nonbeating preparations at room temperature, and the answer to this question must await the refinement of this or other techniques for use in beating mouse hearts. Thus a stimulation of the Na-K-ATPase, a fall in intracellular Na, and a resetting of cellular Ca load by activation of forward mode Na/Ca exchange provide a consistent explanation for a negative inotropic effect of PLM ablation.

Another possibility is that PLM may interact directly with the NCX (1, 22, 27, 29, 31, 33). Cheung and colleagues published a series of studies showing that PLM may colocalize with the NCX and directly regulate its function. Such a direct interaction could underlie changes in contractility in PLM KO myocytes. The association of PLM with both the NCX and the Na-K-ATPase could provide a complex local control of transmembrane Na and Ca transport and contractility. Recent studies by Bossuyt et al. (9), however, used fluorescence resonance energy transfer (FRET) to identify molecular interactions with PLM. FRET was detected between Na-K-ATPase and PLM, suggesting a close coassociation between these two proteins. However, tagging both PLM and NCX proteins with a donor and an acceptor, respectively, did not induce a local FRET signal indicative of molecular proximity. While this suggests a molecular proximity between PLM and Na-K-ATPase, the lack of FRET between the NCX and PLM could be explained by a number of confounding factors and does not rule out an association between these two proteins as reported with coimmunoprecitation (31) and immunofluorescence (33) techniques.

Several studies to date have assessed contractile function in cardiomyocytes with altered PLM expression. In an in vivo study of the PLM KO mouse generated on the noncongenic background, Jia et al. (20) reported a significantly increased ejection fraction in 5-mo-old PLM KO mice. It is unclear whether this reflects the age of the mice, methodological differences (anesthetic heart rate, etc), or the fact that these

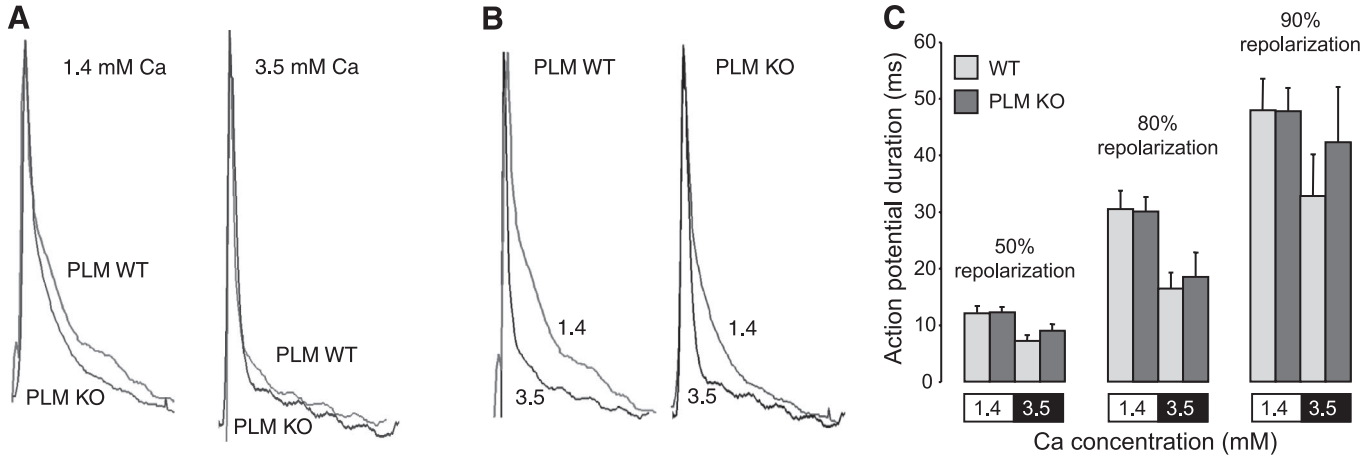

Fig. 3. Monophasic action potentials (MAPs) recorded from the left ventricular free wall of PLM KO and WT hearts. Hearts were paced at 540 beats/min via the ventricle. *A*: representative MAPs from PLM KO and WT hearts at 2 [Ca] (1.4 and 3.5 mM). *B*: MAPs replotted to allow comparison of the effects of Ca within a genotype. *C*: mean action potential durations at 50%, 80%, and 90% repolarization in PLM KO and WT hearts at 2 [Ca] (1.4 and 3.5 mM). Data are means ± SE (n = 6/group).

animals were on the noncongenic background. This latter explanation seems most likely, however, because previous differences between these two PLM KO lines have been reported (33). In isolated myocytes, Mirza et al. (22) used an antisense approach to reduce PLM expression in cultured adult rat myocytes. In cells paced at 1 Hz and treated with antisense PLM, cell shortening was reduced in low $[Ca]_o$ (0.6 mM) and increased in high $[Ca]_o$ (5 mM). The effects in physiological Ca concentrations were not reported. In this study, in unstimulated cells at 30°C in the presence of 5.0 mM extracellular Ca the knockdown of PLM resulted in an increased Na/Ca exchange current compared with green fluorescent protein controls, although this change was minimal over the physiological voltage range and only significant at more positive potentials (22). When overexpressed in cultured adult rat myocytes, PLM had no effect on contractility in the presence of more physiological $[Ca]_o$ (1.8 mM) (27). Tucker et al. (29) more recently reported no differences in cell shortening between myocytes isolated from PLM WT and KO hearts derived from a congenic C57/BL6 background when paced at 1 Hz in the presence of 1.8 mM extracellular Ca. As described for PLM antisense-treated myocytes, contraction amplitude was decreased at low $[Ca]_o$ (0.6 mM) and increased in high $[Ca]_o$ (5 mM) in PLM KO myocytes compared with WT controls.

The substantial and consistent decrease in basal LVDP in the PLM KO Langendorff-perfused heart at 1.4 mM Ca suggests that in the whole heart the slight in vivo contractile deficit is, in fact, even more apparent in vitro. One possible explanation for this is that the PLM KO Langendorff heart is osmotically challenged by crystalloid perfusion. Since PLM has been suggested to play a role in cell volume control, we considered the possibility that a decreased ability of the KO heart to tolerate crystalloid perfusion may contribute to this contractile deficit. However, in separate studies (not shown) we found no substantial differences in the ability of both PLM KO hearts and myocytes to tolerate an hypoosmotic challenge.

The increased Na-K-ATPase activity in PLM KO homogenates presented here is in contrast to that reported previously in noncongenic animals (20). On this noncongenic background, Jia et al. (20) reported that Na-K-ATPase activity normalized for protein expression was slightly reduced in PLM KO hearts. One possible reason for this difference is that we examined the

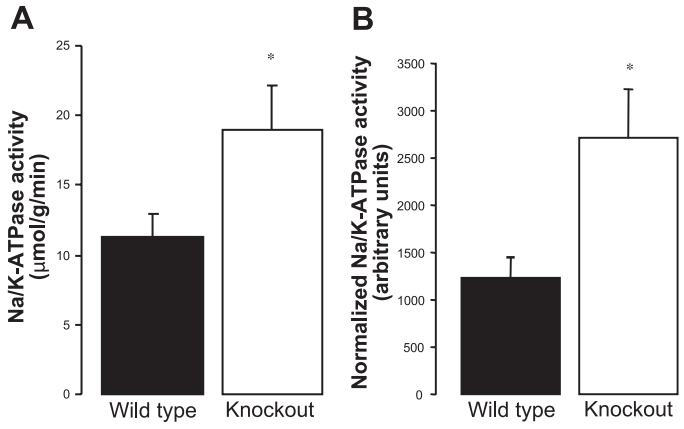

Fig. 4. Ouabain-sensitive Na-K-ATPase activity in crude cardiac homogenates from PLM WT and KO mice. *A*: absolute Na-K-ATPase activity expressed as micromoles of Na-K-ATPase phosphate produced per gram of wet ventricular weight per minute of reaction. *B*: Na-K-ATPase activity normalized to α_1-subunit expression. Data are means ± SE (WT n = 7, KO n = 5). *$P < 0.05$.

Table 3. *Expression of proteins from Na-K-ATPase pump complex and other proteins involved in excitation-contraction coupling in PLM KO and WT ventricle*

	WT	PLM KO	P Value
PLM	2,993±212	0±0	
Na-K-ATPase α_1-subunit	1,561±156	1,124±164	ns
Na-K-ATPase α_2-subunit	1,890±157	1,888±273	ns
Na-K-ATPase β_1-subunit	1,527±128	1,248±158	ns
Na-K-ATPase β_2-subunit	1,959±259	1,593±126	ns
SERCA2a	1,330±285	1,036±247	ns
PLB	1,574±348	2,305±547	ns
NCX	1,476±396	1,561±207	ns

Data are means ± SE (n = 8). Protein expression is expressed in arbitrary densitometric units. SERCA, sarco(endo)plasmic reticulum Ca-ATPase; PLB, phospholamban; NCX, Na/Ca exchanger. With the exception of PLM, there were no changes in the expression of the other major Na-K-ATPase subunits or other major Ca-handling proteins.

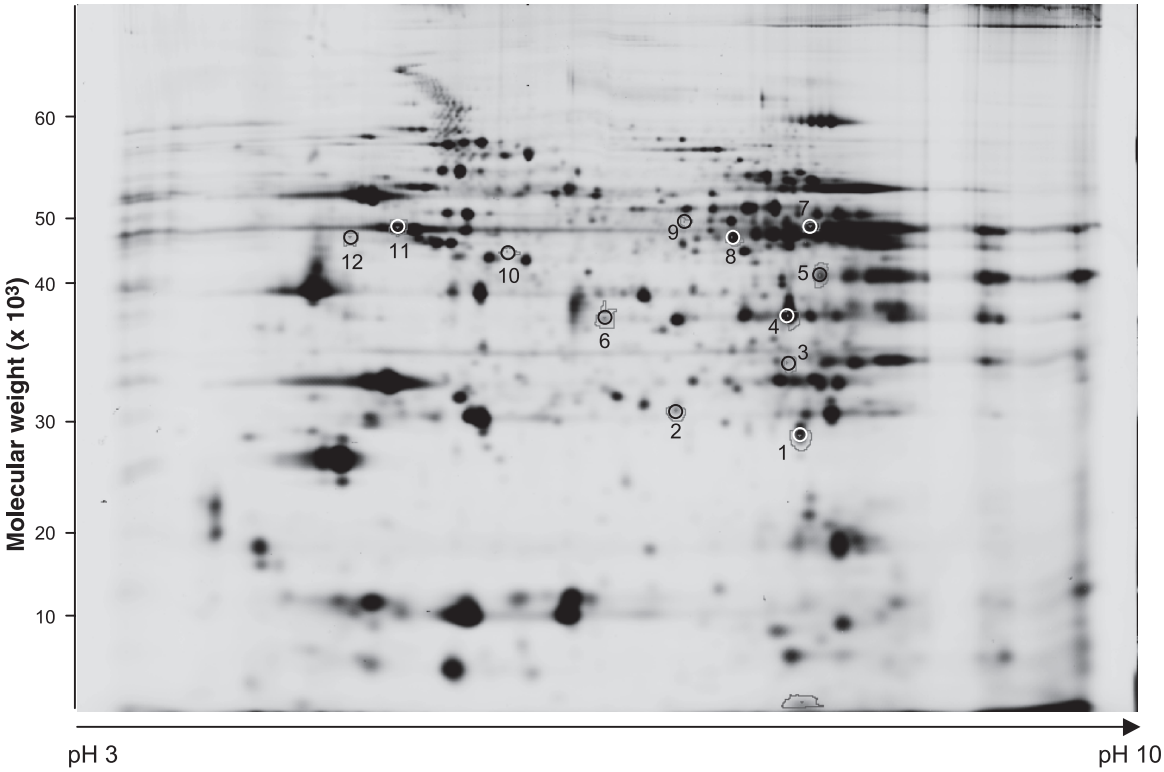

Fig. 5. Two-dimensional electrophoresis of PLM WT and KO hearts. Differential gel electrophoresis (DIGE)-labeled proteins were focused according to isoelectric point in first-dimension isoelectric focusing on 24-cm NL pH 3–10 IPG strips. Focused strips were then separated according to molecular weight by 2-dimensional electrophoresis on 12% polyacrylamide slab gels. Gels were then scanned with the Typhoon 9400 variable-mode imager. Proteins of interest, determined by DeCyder expression analysis ($P < 0.05$, $n = 5$), are circled and numbered. Protein identifications can be seen in Table 4.

ouabain-sensitive fraction of a crude cardiac homogenate while the study of Jia et al. (20) used membranes purified by sucrose gradient. Both approaches have their limitations; the crude homogenate has only a small ouabain-sensitive ATPase fraction (~6–10%), while we have found sucrose gradients unsuitable for use in cardiac tissue. While the membrane fraction obtained from such a gradient interface represents a purer preparation, it also only constitutes a very small subpopulation

Table 4. *Identification of proteins with modulated expression in PLM KO hearts compared with WT controls*

Sample Number	Protein Description	Accession No.	MW (×10³)	Peptides	General Function	Avg Ratio	*P* Value
1	NADH-ubiquinone oxidoreductase	Q90059	35.9	2	Mitochondrial complex I electron acceptor	−1.20	0.0022
2	ATP synthase α	Q03265	59.8	9	Mitochondrial ATP synthesis	+1.35	0.049
3	Adenylate kinase	Q9WUR9	25.1	8	Mitochondrial ATP production from ADP	+1.16	0.0047
4	Electron transfer flavoprotein α-subunit	Q8BMD3	35.0	10	Mitochondrial electron transport	+1.06	0.038
5	GAPDH	P16858	35.7	5	Carbohydrate metabolism	−1.14	0.0055
	Aldolase reductase	P45376	35.6	3	Catalyzes NADPH-dependent reduction of carbonyl compounds		
6	δ, 3,5-δ-2,4-Dionyl CoA tisomerase	O35459	36.1	11	Mitochondrial fatty acid β-oxidation cycle	−1.13	0.014
7	3-Ketoacyl CoA thiolase	P13437	41.9	11	Mitochondrial fatty acid metabolism	−1.11	0.0033
	Creatine kinase	P09605	47.4	12	Mitochondrial energy transduction		
	Phosphoglycerate kinase	P09411	44.4	8	Cytoplasmic ATP production in glycolysis		
8	Isovaleryl-CoA dehydrogenase	P26440	46.3	10	Mitochondrial leucine catabolism	+1.07	0.043
9	Elongation factor	P49411	49.5	10	Protein synthesis (mitochondria)	−1.38	0.017
10	Ubiquinol cytochrome *c* reductase	Q9CZ13	52.8	6	Electron transferring protein in mitochondrial respiratory chain	+1.54	0.0036
11	Actin	P12718	41.9	8	Structure/cytoskeleton	−1.16	0.035
12	Desmin	P31001	53.4	3	Structure/cytoskeleton	+1.36	0.038

Hearts were Langendorff perfused ($n = 5$), homogenized, and subjected to a standard 2-dimensional electrophoresis (isoelectric focusing, SDS-PAGE), as described in MATERIALS AND METHODS. Proteins found to have significantly altered expression were tryptically digested and identified with an Applied Biosystems 4700 Proteomics Analyzer MALDI-TOF-TOF mass spectrometer, using 10 mg/ml α-cyano-4-hydroxycinnamic acid as the matrix. Sample number refers to the hits identified on Fig. 5, with the identity of the corresponding protein(s) presented. Note that *samples 5* and *7* contained >1 protein. Included are each protein's UniProt accession number and the number of peptides matched for each hit. Ratios refer to the fold changes in up-/downregulation in protein expression, with the corresponding *P* value. MW, molecular weight.

of the total Na-K-ATPase of the myocyte. In both qualitative and quantitative agreement with the measurements made in the present study, using a different approach we have used whole cell voltage clamping to show that PLM deletion approximately doubles the normalized Na-K pump current (7).

Protein analyses suggest the deletion of PLM is the predominant cause of the phenotypic differences between PLM WT and KO hearts. The small, nonsignificant decrease in Na-K-ATPase α_1-subunit expression observed here by SDS-PAGE and Western blotting is similar to the decrease reported previously (13, 29), possibly reflecting a compensatory change to offset the increased Na-K-ATPase activity in the absence of PLM. A more in depth analysis with two-dimensional electrophoresis (IEF, SDS-PAGE) showed minimal changes in protein expression in the PLM KO hearts, with high-abundance mitochondrial proteins constituting the majority of these changes.

In summary, we have provided evidence for a role for PLM in regulating the contractile function of the normoxic mouse heart. A depressed contractile function in PLM KO hearts exhibiting a significantly raised Na-K-ATPase activity is in agreement with recently published reports of an inhibitory action of PLM on the Na-K-ATPase and suggests that PLM, as a major target of β-adrenergic-activated kinases, may be involved in the series of events contributing to the modulation of cardiac contractile function.

ACKNOWLEDGMENTS

Present addresses: J. R. Bell, Cardiac Phenomics Laboratory, Dept. of Physiology, University of Melbourne, Melbourne, VIC 3010, Australia; W. Fuller, Institute of Cardiovascular Research, Vascular and Inflammatory Diseases Research Unit, Dept. of Medicine, Ninewells Hospital and Medical School, Dundee DD1 9SY, UK.

GRANTS

This study was supported by grants from the British Heart Foundation and the Medical Research Council to M. J. Shattock, M. S. Marber, and J. E. Clark and to M. J. Dunn from the British Heart Foundation and the Science Foundation Ireland (04/RPI/B499).

REFERENCES

1. **Ahlers BA, Zhang XQ, Moorman JR, Rothblum LI, Carl LL, Song J, Wang J, Geddis LM, Tucker AL, Mounsey JP, Cheung JY.** Identification of an endogenous inhibitor of the cardiac Na^+/Ca^{2+} exchanger, phospholemman. *J Biol Chem* 280: 19875–19882, 2005.
2. **Baginski ES, Foa PP, Zak B.** Microdetermination of inorganic phosphate, phospholipids, and total phosphate in biologic materials. *Clin Chem* 13: 326–332, 1967.
3. **Beguin P, Crambert G, Guennoun S, Garty H, Horisberger JD, Geering K.** CHIF, a member of the FXYD protein family, is a regulator of Na,K-ATPase distinct from the γ-subunit. *EMBO J* 20: 3993–4002, 2001.
4. **Beguin P, Crambert G, Monnet-Tschudi F, Uldry M, Horisberger JD, Garty H, Geering K.** FXYD7 is a brain-specific regulator of Na,K-ATPase α_1-β isozymes. *EMBO J* 21: 3264–3273, 2002.
5. **Beguin P, Wang X, Firsov D, Puoti A, Claeys D, Horisberger JD, Geering K.** The γ subunit is a specific component of the Na,K-ATPase and modulates its transport function. *EMBO J* 16: 4250–4260, 1997.
6. **Berry RG.** *Regulation of Na/K Pump Current in Isolated Cardiac Myocytes: Studies in the Phospholemman Knockout Mouse* (PhD thesis). London: University of London, 2007.
7. **Berry RG, Fuller W, Shattock MJ.** Regulation of cardiac Na/K-ATPase by FXYD1 (phospholemman) (Abstract). *J Mol Cell Cardiol* 40: 997 (A212), 2006.
8. **Bers DM.** Cardiac Na/Ca exchange function in rabbit, mouse and man: what's the difference? *J Mol Cell Cardiol* 34: 369–373, 2002.
9. **Bossuyt J, Despa S, Martin JL, Bers DM.** Phospholemman phosphorylation alters its fluorescence resonance energy transfer with the Na/K-ATPase pump. *J Biol Chem* 281: 32765–32773, 2006.
10. **Boulanger-Saunier C, Stoclet JC.** A 16 kDa protein substrate for protein kinase C and its phosphorylation upon stimulation of vasopressin receptors in rat aortic myocytes. *Biochem Biophys Res Commun* 143: 517–524, 1987.
11. **Bradford MM.** A rapid and sensitive method for the quantitation of microgram quantities of protein utilizing the principle of protein-dye binding. *Anal Biochem* 72: 248–254, 1976.
12. **Choisy SC, Arberry LA, Hancox JC, James AF.** Increased susceptibility to atrial tachyarrhythmia in spontaneously hypertensive rat hearts. *Hypertension* 49: 498–505, 2007.
13. **Despa S, Bossuyt J, Han F, Ginsburg KS, Jia LG, Kutchai H, Tucker AL, Bers DM.** Phospholemman-phosphorylation mediates the β-adrenergic effects on Na/K pump function in cardiac myocytes. *Circ Res* 97: 252–259, 2005.
14. **Donoghue PM, McManus CA, O'Donoghue NM, Pennington SR, Dunn MJ.** CyDye immunoblotting for proteomics: co-detection of specific immunoreactive and total protein profiles. *Proteomics* 6: 6400–6404, 2006.
15. **Fuller W, Eaton P, Bell JR, Shattock MJ.** Ischemia-induced phosphorylation of phospholemman directly activates rat cardiac Na/K-ATPase. *FASEB J* 18: 197–199, 2004.
16. **Fuller W, Eaton P, Medina RA, Bell J, Shattock MJ.** Differential centrifugation separates cardiac sarcolemmal and endosomal membranes from Langendorff-perfused rat hearts. *Anal Biochem* 293: 216–223, 2001.
17. **Fuller W, Shattock MJ.** Phospholemman (FXYD1) is a substrate for multiple protein kinases in vitro (Abstract). *Biophys J* 88: 2946-Pos, 2005.
18. **Görg A, Postel W, Günther S, Weser J, Strahler JR, Hanash SM, Somerlot L, Kuick R.** Approach to stationary two-dimensional pattern: influence of focusing time and immobiline/carrier ampholytes concentrations. *Electrophoresis* 9: 37–46, 1988.
19. **Han F, Bossuyt J, Despa S, Tucker AL, Bers DM.** Phospholemman phosphorylation mediates the protein kinase C-dependent effects on Na^+/K^+ pump function in cardiac myocytes. *Circ Res* 99: 1376–1383, 2006.
20. **Jia LG, Donnet C, Bogaev RC, Blatt RJ, McKinney CE, Day KH, Berr SS, Jones LR, Moorman JR, Sweadner KJ, Tucker AL.** Hypertrophy, increased ejection fraction, and reduced Na-K-ATPase activity in phospholemman-deficient mice. *Am J Physiol Heart Circ Physiol* 288: H1982–H1988, 2005.
21. **Lu KP, Kemp BE, Means AR.** Identification of substrate specificity determinants for the cell cycle-regulated NIMA protein kinase. *J Biol Chem* 269: 6603–6607, 1994.
22. **Mirza MA, Zhang XQ, Ahlers BA, Qureshi A, Carl LL, Song J, Tucker AL, Mounsey JP, Moorman JR, Rothblum LI, Zhang TS, Cheung JY.** Effects of phospholemman downregulation on contractility and $[Ca^{2+}]_i$ transients in adult rat cardiac myocytes. *Am J Physiol Heart Circ Physiol* 286: H1322–H1330, 2004.
23. **Presti CF, Jones LR, Lindemann JP.** Isoproterenol-induced phosphorylation of a 15-kilodalton sarcolemmal protein in intact myocardium. *J Biol Chem* 260: 3860–3867, 1985.
24. **Presti CF, Scott BT, Jones LR.** Identification of an endogenous protein kinase C activity and its intrinsic 15-kilodalton substrate in purified canine cardiac sarcolemmal vesicles. *J Biol Chem* 260: 13879–13889, 1985.
25. **Rembold CM, Ripley ML, Meeks MK, Geddis LM, Kutchai HC, Marassi FM, Cheung JY, Moorman JR.** Serine 68 phospholemman phosphorylation during forskolin-induced swine carotid artery relaxation. *J Vasc Res* 42: 483–491, 2005.
26. **Silverman BZ, Fuller W, Eaton P, Deng J, Moorman JR, Cheung JY, James AF, Shattock MJ.** Serine 68 phosphorylation of phospholemman: acute isoform-specific activation of cardiac Na/K ATPase. *Cardiovasc Res* 65: 93–103, 2005.
27. **Song J, Zhang X, Carl LL, Qureshi A, Rothblum LI, Cheung JY.** Overexpression of phospholemman alters contractility and $[Ca^{2+}]_i$ transients in adult rat myocytes. *Am J Physiol Heart Circ Physiol* 283: H576–H583, 2002.
28. **Therien AG, Karlish SJ, Blostein R.** Expression and functional role of the gamma subunit of the Na,K-ATPase in mammalian cells. *J Biol Chem* 274: 12252–12256, 1999.
29. **Tucker AL, Song J, Zhang XQ, Wang J, Ahlers BA, Carl LL, Mounsey JP, Moorman JR, Rothblum LI, Cheung JY.** Altered contractility and $[Ca^{2+}]_i$ homeostasis in phospholemman-deficient murine myocytes: role of Na^+/Ca^{2+} exchange. *Am J Physiol Heart Circ Physiol* 291: H2199–H2209, 2006.

30. **Walaas O, Horn RS, Walaas SI.** Inhibition of insulin-stimulated phosphorylation of the intracellular domain of phospholemman decreases insulin-dependent GLUT4 translocation in streptolysin-O-permeabilized adipocytes. *Biochem J* 343: 151–157, 1999.
31. **Wang J, Zhang XQ, Ahlers BA, Carl LL, Song J, Rothblum LI, Stahl RC, Carey DJ, Cheung JY.** Cytoplasmic tail of phospholemman interacts with the intracellular loop of the cardiac Na^+/Ca^{2+} exchanger. *J Biol Chem* 281: 32004–32014, 2006.
32. **Weekes J, Wheeler CH, Yan JX, Weil J, Eschenhagen T, Scholtysik G, Dunn MJ.** Bovine dilated cardiomyopathy: proteomic analysis of an animal model of human dilated cardiomyopathy. *Electrophoresis* 20: 898–906, 1999.
33. **Zhang XQ, Qureshi A, Song J, Carl LL, Tian Q, Stahl RC, Carey DJ, Rothblum LI, Cheung JY.** Phospholemman modulates Na^+/Ca^{2+} exchange in adult rat cardiac myocytes. *Am J Physiol Heart Circ Physiol* 284: H225–H233, 2003.